HHS Public Access

Author manuscript

Hepatology. Author manuscript; available in PMC 2019 June 01.

Published in final edited form as:

Hepatology. 2018 June ; 67(6): 2150–2166. doi:10.1002/hep.29676.

Modulation of the intestinal bile acid–FXR–FGF15 axis improves alcoholic liver disease in mice

Phillipp Hartmann[1,2], **Katrin Hochrath**[1], **Angela Horvath**[1,3], **Peng Chen**[1], **Caroline T. Seebauer**[1], **Cristina Llorente**[1,4], **Lirui Wang**[1,4], **Yazen Alnouti**[5], **Derrick E. Fouts**[6], **Peter Stärkel**[7], **Rohit Loomba**[1], **Sally Coulter**[8], **Christopher Liddle**[8], **Ruth T. Yu**[9], **Lei Ling**[10], **Stephen J. Rossi**[10], **Alex M. DePaoli**[10], **Michael Downes**[9], **Ronald M. Evans**[9,11], **David A. Brenner**[1], and **Bernd Schnabl**[1,4]

[1]Department of Medicine, University of California San Diego, La Jolla, CA, USA

[2]Department of Pediatrics, University of California San Diego, La Jolla, CA, USA

[3]Department of Gastroenterology and Hepatology, Medical University of Graz, Graz Austria

[4]Department of Medicine, VA San Diego Healthcare System, San Diego, CA, USA

[5]Department of Pharmaceutical Sciences, University of Nebraska Medical Center, Omaha, NE, USA

[6]J. Craig Venter Institute, Rockville, MD, USA

[7]St. Luc University Hospital, Université Catholique de Louvain, Brussels, Belgium

[8]Storr Liver Centre, Westmead Institute for Medical Research and Sydney Medical School, University of Sydney, Australia

[9]Gene Expression Laboratory, Salk Institute for Biological Studies, La Jolla, California, USA

[10]NGM Biopharmaceuticals, Inc., South San Francisco, CA, USA

[11]Howard Hughes Medical Institute, Salk Institute for Biological Studies, La Jolla, CA, USA

Abstract

Alcoholic liver disease is associated with changes in the intestinal microbiota. Functional consequences of alcohol-associated dysbiosis are largely unknown. The aim of this study was to identify a mechanism of how changes in the intestinal microbiota contribute to alcoholic liver disease. Metagenomic sequencing of intestinal contents demonstrated that chronic ethanol feeding in mice is associated with an overrepresentation of bacterial genomic DNA encoding choloylglycine hydrolase, which deconjugates bile acids in the intestine. Bile acid analysis confirmed an increased amount of unconjugated bile acids in the small intestine after ethanol administration. Mediated by a lower farnesoid x receptor (FXR) activity in enterocytes, lower fibroblast growth factor (FGF)-15 protein secretion was associated with increased hepatic

Correspondence: Bernd Schnabl, M.D., Department of Medicine, University of California San Diego, MC0063, 9500 Gilman Drive, La Jolla, CA 92093, Phone 858-822-5311, Fax 858-822-5370, beschnabl@ucsd.edu.

Conflict of interest: L.L., S.J.R. and A.M.D. are employees and stockholders of NGM Biopharmaceuticals Inc. M.D. and R.M.E. are co-inventors of FXR molecules and methods of use and may be entitled to royalties.

cytochrome P450 enzyme (Cyp)-7a1 protein expression and circulating bile acid levels. Depletion of the commensal microbiota with non-absorbable antibiotics attenuated hepatic Cyp7a1 expression and reduced alcoholic liver disease in mice, suggesting that increased bile acid synthesis is dependent on gut bacteria. To restore intestinal FXR activity, we used a pharmacological intervention with the intestine-restricted FXR agonist fexaramine, which protected mice from ethanol-induced liver injury. While bile acid metabolism was only minimally altered, fexaramine treatment stabilized the gut barrier and significantly modulated hepatic genes involved in lipid metabolism. To link the beneficial metabolic effect to FGF15, a non-tumorigenic FGF19 variant – a human FGF15 ortholog – was overexpressed in mice using adeno-associated viruses. FGF19 treatment showed similarly beneficial metabolic effects and ameliorated alcoholic steatohepatitis. Taken together, alcohol-associated metagenomic changes result in alterations of bile acid profiles. Targeted interventions improve bile acid–FXR–FGF15 signaling by modulation of hepatic Cyp7a1 and lipid metabolism, and reduce ethanol-induced liver disease in mice.

Keywords

bile acids; microbiome; metagenome

Introduction

Alcohol abuse is the cause for cirrhosis in 50% of patients with end-stage liver disease (1). Chronic alcohol use is linked to changes in the intestinal microbiota in preclinical models (2–4) and humans (5, 6). Alcohol exposure/use oftentimes leads to small intestinal bacterial overgrowth (3, 7). Recent studies evaluated the link between changes in the microbiota composition and alcoholic liver disease progression. Dysbiosis contributes to increased intestinal permeability, which allows microbial products to translocate from the intestinal lumen to the liver (8, 9). Pathogen associated microbial patterns (PAMPs) bind to pathogen recognition receptors in the liver to increase liver inflammation and hepatocyte death (10, 11). Beyond changes in gut barrier function, chronic ethanol administration also changes the function of the intestinal microbiota. The biosynthesis of saturated fatty acids is decreased in intestinal bacteria, which contributes to gut barrier dysfunction (12).

Bile acids are synthesized, conjugated to glycine or taurine in hepatocytes, and secreted via the biliary system into the duodenum. Conjugated bile acids are present in mixed micelles and have lipid emulsifying functions. Conjugated bile acids are absorbed via the apical sodium dependent bile acid transporter (ASBT) into enterocytes of the distal ileum. Conjugated bile acids bind to farnesoid x receptor (FXR) in the intestine to induce endocrine hormone fibroblast growth factor (FGF)-15 (FGF19 in humans), which decreases the transcription of cytochrome P450 enzyme (Cyp)7a1 in hepatocytes thereby limiting de novo synthesis of bile acids (13, 14). Primary conjugated bile acids are dehydroxylated and deconjugated by intestinal bacteria in the colon and the small intestine (15). Secondary bile acids are then absorbed (predominantly) passively and can return to the liver via the enterohepatic circulation. FGF19 lowers body weight and protects from diet-induced obesity by suppressing hepatic lipogenesis and increasing hepatic fatty acid oxidation (16).

Germfree mice show alterations in their bile acid profiles supporting an important role of the gut microbiota for bile acid metabolism (17). Chronic alcohol consumption is associated with changes in bile acid profiles in patients. Serum conjugated deoxycholic acid (DCA) and chenodeoxycholic acid (CDCA) were increased and decreased, respectively, in active drinkers without liver disease as compared with healthy controls (18). Total and secondary bile acids were increased in fecal samples of active drinkers (18).

Using metagenomics and bile acid analysis we investigated the effects of chronic ethanol administration on the metabolic function of the intestinal microbiota.

Materials and Methods

Mice

Wild-type C57BL/6 mice (Charles River) were fed a Lieber DeCarli alcohol or isocaloric control diet for 8 weeks starting at 8–10 weeks of age. The Lieber DeCarli alcohol diet consisted of Micro Stabilized Rod Liq AC IRR (LD101A) (and Maltodextrin IRR (9598) for the first week) from TestDiet (St. Louis, MO) and 200 Proof Ethanol from Gold Shield (Hayward, CA) in a specific combination following the manufacturer's feeding directions. In brief, the caloric intake from ethanol was 0% on day 1, 10% on day 2 and 3, 20% on day 4 and 5, 30% from day 6 until the end of 6 weeks, and 36% for the last 2 weeks. Mortality of alcohol-fed mice was less than 25% in each ethanol-fed group. Pair-fed control mice received a diet with an isocaloric substitution of dextrose (LD101; TestDiet, St. Louis, MO).

For the antibiotics study, antibiotics treatment was started at 4 weeks after start of liquid diet feeding, and mice were gavaged daily until harvesting. The composition of the antibiotics mixture has been described (polymyxin B (150mg/kg BW/day) and neomycin (200mg/kg BW/day)) (8). Fexaramine was synthesized following the protocol outlined in Nicolaou et al. (19), by TBJ (San Diego, CA) chemical consultant company. The structure and purity of fexaramine (≥98.0%) were confirmed by nuclear magnetic resonance (NMR), high-performance liquid chromatography (HPLC), and liquid chromatography/mass spectrometry (LC-MS) analyses, as well as by carbon, hydrogen and nitrogen elemental analyses. Fexaramine (100mg/kg BW) was diluted in corn oil and gavaged daily during 8 weeks of alcohol feeding. Corn oil served as vehicle control. For the AAV-M52 study, an adeno-associated virus (AAV; AAV2/9 serotype with EF1a promoter, NGM Biopharmaceuticals, San Francisco, CA) expressing the human non-tumorigenic FGF19-variant M52 (US patent US8951966B2) was injected into mice. 3×10^{11} v.g. AAV per mouse were injected once into the tail vein in a volume of 100μL per mouse. AAV expressing green fluorescent protein (GFP, NGM Biopharmaceuticals, San Francisco, CA) was used as control. AAV was injected 3 weeks after isocaloric or ethanol feeding was started. Age-matched female mice were used throughout the experiments. All animal studies were reviewed and approved by the Institutional Animal Care and Use Committee of the University of California, San Diego.

Metagenomic sequencing

High molecular weight genomic DNA was extracted and purified from the ceca of alcohol and control animals (3). Metagenomic sequencing and analysis was performed as described

(12). In brief, shotgun libraries were sequenced using an Illumina HiSeq 2000 platform (San Diego, CA). After removing reads matching the MGSCv37/mm9 mouse genome assembly, filtered sequences were assembled into contigs and uploaded to the Metagenomics Analysis Server (MG-RAST) at metagenomics.anl.gov for annotation and metabolic reconstruction (20). The MG-RAST KEGG Mapper was used under default settings to display differential abundances of enzymes involved in metabolism. Data can be accessed through MG-RAST. Sequence reads have been deposited under NCBI BioSamples SAMN02671702-SAMN02671718 under BioProject PRJNA89097(12).

Bile acid quantification

Bile acids in liver, plasma, intestinal contents, urine and feces in wild-type mice fed an isocaloric or ethanol containing diet for 8 weeks as well as bile acids in intestinal contents in fexaramine- (or corn oil-) treated mice were quantified by LC-MS as described (21–23). Fecal samples and intestinal contents were dried, and equal amounts were processed. Bile acid analysis of plasma samples of mice treated with antibiotics or fexaramine was performed as follows. Serum (20 μl) was protein precipitated with 80 μl of cold acetonitrile containing deuterated cholic acid as an internal standard, vortexed for 1 min and centrifuged at 10,000 rpm for 10 min at 4°C. Supernatant was evaporated under vacuum and reconstituted in assay mobile phase. Bile acid separation was achieved using an Acuity (Waters, Milford, MA) UPLC BEH C18 column (1.7microns 2.1×100mm) on a Nextera UPLC (Shimadzu, Tokyo, Japan); the temperature of the column and auto sampler was 65°C and 12°C, respectively. Sample injection volume was 1μl. The mobile phase consisted of 10% acetonitrile and 10% methanol in water containing 0.1% formic acid (Mobile Phase A) and 10% methanol in acetonitrile 0.1% formic acid (Mobile Phase B) delivered as a gradient: 0–5 min Mobile Phase B held at 22%; 5–12 min Mobile Phase B increased linearly to 60%, 12–15min Mobile Phase B increased linearly to 80% and 15–19 min Mobile Phase B constant at 80% at a flow rate of 0.5ml/min. The mass spectrometer (Q-Trap 5500; Sciex, Framingham, MA) was operated in negative electro-spray mode working in the multiple reaction mode (MRM). Operating parameters were: curtain gas 30psi; ion spray voltage 4500 V; temperature 550°C; ion source gas 1 60psi; ion source gas 2 65psi. Transition MRMs, declustering potential, entrance potentials and collision cell exit potentials were optimized using the Analyst software (Sciex, Framingham, MA). Dwell times were 25msec.

RNA sequencing

RNA was extracted from mouse tissue using Trizol (Invitrogen, Carlsbad, CA). RNA was digested with DNase using the DNA-free DNA removal kit (Ambion, Carlsbad, CA). Library generation and sequencing was performed as described (24). In brief, sequencing libraries were prepared from total RNA using the TruSeq RNA Sample Preparation Kit v2 (Illumina, San Diego, CA) followed by 100bp single ended sequencing on the Illumina HiSeq 2500. Image analysis and base calling were performed with Illumina CASAVA-1.8.2, while read alignment and junction finding was accomplished using STAR (25). Gene expression analysis, statistical testing and annotation was performed using Cuffdiff 2 (26), utilizing UCSC GRCm38/mm10 as the reference assembly. Transcript expression was calculated as gene-level relative abundance in fragments per kilobase of exon model per million mapped fragments and employed correction for transcript abundance bias (27).

RNA-Seq data reported in this paper have been deposited in the National Center for Biotechnology Information (NCBI) Sequence Read Archive (SRA) database, Accession # SRP100462.

Statistical analysis

The unpaired Student's t-test was used for statistical analysis for all graphs where only two groups were being compared, or analysis of variance (ANOVA) followed by the Newman-Keuls test for comparison of more than two groups (Prism, GraphPad Software, La Jolla, CA). Results are presented as mean ± SEM. A P value < 0.05 was selected as the level of significance.

Other materials and methods are described in the Supplementary Materials and Methods section.

Results

Chronic ethanol feeding disrupts the enterohepatic circulation of bile acids and reduces intestinal FXR activity

To determine functional differences of the intestinal microbiota, metagenomic sequencing was performed following chronic ethanol feeding. Metagenomic analysis revealed that bacterial genomic DNA encoding choloylglycine hydrolase (CGH; [EC 3.5.1.24]) is more abundant in intestinal contents of mice fed ethanol than in controls (Fig. 1A). Bacterial choloylglycine hydrolase is responsible for the deconjugation (deamidation) of conjugated (amidated) bile acids (Fig. 1A) (28). Based on our sequencing results, choloylglycine hydrolase was mainly expressed in *Lactobacillus, Lactococcus, Bacteroides*, and *Pediococcus*. As we have published, the metagenomic dataset also demonstrated reduced levels of the FabG, FabF, and FabD genes (Fig. 1A), which are involved in fatty acid metabolism (12).

To assess whether changes in the metagenome associated with chronic alcohol feeding directly translate into changes of bile acid profiles, bile acid analysis using mass spectrometry were performed. Enhanced deconjugation increased levels of unconjugated bile acids in the ileum in ethanol-fed mice compared with controls (Fig. 1B). In particular, the proportions of taurine conjugated cholic acid (TCA) and deoxycholic acid (TDCA) decreased, while cholic acid (CA), total muricholic acid (MCA) and deoxycholic acid (DCA) increased in the ileum after ethanol administration (Fig. 1C). Deconjugated bile acids – in particular monohydroxy and most dihydroxy bile acids – are rapidly absorbed mostly by nonionic diffusion in the intestine leading to augmented unconjugated and total bile acid concentrations in the plasma of alcohol fed mice (Fig. 1D). Following reuptake into hepatocytes, unconjugated bile acids are rapidly conjugated, resulting in significantly higher hepatic concentrations of conjugated and total bile acids after chronic ethanol feeding (Fig. 1D). Similarly, the concentration of bile acids in the gallbladder (Fig. 1E) and the gallbladder weight (Suppl. Fig. 1A) were elevated in the alcohol-fed group. Gallbladder bile acid composition was not changed by alcohol feeding (Suppl. Fig. 1B). Amounts and composition of fecal bile acids were similar between isocaloric and ethanol fed mice as were

urine bile acids (Fig. 1F, Suppl. Fig 1C). Alcohol feeding also resulted in an increased total bile acid pool (Fig. 1G). FXR activity can be induced by conjugated bile acids (29) and – to some degree – by TCA (30). Likely mediated by a lower FXR activity in enterocytes of the terminal ileum resulting from a lower percentual concentration of conjugated bile acids and the significantly lower TCA in the ileum, less FGF15 protein was detected in the ileum (Suppl. Fig 2) and secreted into the plasma of ethanol-fed mice (Fig. 1H). As the rate-limiting enzyme for bile acid synthesis in the liver, Cyp7a1, is regulated by negative feedback mechanism via FGF15 (31). We observed increased hepatic Cyp7a1 protein expression (Fig. 1I), which likely contributes to increased total plasma and hepatic bile acids following chronic ethanol feeding (Fig. 1D). Protein expression of other enzymes involved in bile acid synthesis, Cyp8b1 and Cyp27a1, were not affected by alcohol feeding (Suppl. Fig. 3A). Conjugated bile acids activate the sphingosine-1-phosphate receptor 2, which activates Akt and Erk1/2 signaling pathways (32). Although hepatic bile acid composition changed, phosphorylation of Erk1/2 and Akt in the liver was not altered following chronic ethanol administration (Suppl. Fig. 3B). Alkaline phosphatase (not shown) and total bilirubin concentrations (Suppl. Fig. 3C) were not increased in the alcohol-fed group when compared with the isocaloric control group, indicating absence of cholestasis in ethanol treated mice. Hepatic bile acid transporters such as *Ntcp* or *Bsep* as well as intestinal bile acid transporters such as *Asbt* were not affected by alcohol feeding (Suppl. Fig. 4A – 4B). Thus, chronic ethanol administration disrupts the negative feedback loop on bile acid synthesis, and despite elevated systemic bile acids, hepatocytes continue to generate bile acids. In addition, changes in the bile acid composition are observed after chronic ethanol feeding.

Disruption of the enterohepatic circulation depends on the intestinal microbiome in alcoholic liver disease

We then attempted to restore bile acid homeostasis. Our first approach was to target intestinal dysbiosis and to eradicate commensal microbes in the intestine with non-absorbable antibiotics. We have previously reported that polymyxin B and neomycin abolished intestinal bacterial overgrowth, decreased liver injury and steatosis, but did not affect intestinal absorption of ethanol (8). Here we demonstrate that oral antibiotics decreased hepatic Cyp7a1 expression (Fig. 2A) and restored systemic, i.e. plasma, bile acid levels (Fig. 2B). In addition to reversing increased total plasma bile acids following chronic ethanol feeding, antibiotics had a profound effect on plasma bile acid composition following chronic ethanol administration. In particular, there was a general increase in conjugated bile acids and in particular an increase of taurine-conjugated CA and taurine-conjugated beta-MCA (Fig. 2C). Inhibition of intestinal FXR resulted in decreased ceramide signaling in a high-fat diet-induced NAFLD mouse model. This downregulated hepatic fatty acid synthesis–related genes, such as sterol response element–binding protein 1c (Srebp1c) and DNA fragmentation factor α-like effector A (Cidea), leading to reduced hepatic steatosis (30). *Srebp1* and *Cidea* gene expression was not affected by antibiotics (Suppl. Fig. 5). These results support our metagenomic and bile acid analysis and suggest that increased bile acid synthesis is dependent on the intestinal microbiome. Furthermore, the known beneficial effect of intestinal decontamination on alcoholic liver disease might not only be mediated by

reducing intestinal bacterial overgrowth and translocation of bacterial products, but also by changing plasma bile acid profiles.

The intestine-restricted FXR agonist fexaramine alleviates ethanol-induced liver disease

Our findings suggest that chronic ethanol intake induces dysbiosis and modulates bile acids, resulting in lower intestinal FXR signaling and increased plasma bile acids. Our second intervention approach aimed at restoring intestinal FXR signaling. We therefore investigated whether treating mice with an intestine-specific FXR agonist prevents ethanol-associated liver disease in mice. We used the synthetic FXR agonist fexaramine, which is not absorbed after oral gavage and does not show systemic FXR stimulation (24). Daily gavage of fexaramine reduced ethanol-induced liver injury (as demonstrated by lower plasma ALT levels) and steatosis (Fig. 3A – 3D). Ethanol-induced hepatic inflammation as evidenced by increased hepatic interleukin (IL1)B and tumor necrosis factor (TNF) protein, was decreased in the liver of fexaramine-treated mice (Fig. 3E – 3F).

After absorption in the gastrointestinal tract, ethanol is metabolized in the liver via alcohol-dehydrogenase 1 (*Adh1*) and the inducible Cyp2e1. Intestinal ethanol absorption or hepatic ethanol metabolism by *Adh1* and Cyp2e1 was not affected after activation of FXR in the intestine (Suppl. Fig. 6A – 6C).

FXR induces antimicrobial molecules in intestinal epithelial cells (29) and protects from intestinal barrier dysfunction (24). Fexaramine did not affect the total amount of bacteria in the cecum after ethanol administration (Suppl. Fig. 7A). Ethanol is known to disrupt enteric tight junctions and to induce intestinal barrier dysfunction (33). We have confirmed this by measuring fecal albumin and the intestinal tight junction protein occludin (Suppl. Fig. 7B – 7C). Fexaramine treatment maintained intestinal barrier integrity, as determined by reduced fecal albumin levels and a higher intestinal occludin protein expression than vehicle treated mice after ethanol feeding (Suppl. Fig. 7B – 7C). This is associated with lower inflammatory cytokine expression such as *Tnf* and *Il1b* in the ileum (Suppl Fig. 7D). Dysbiosis-induced intestinal inflammation mediated by TNF is known to disrupt the intestinal barrier and to contribute to alcoholic liver disease (8). It is therefore possible that fexaramine-induced FXR activity, as evidenced by increased Shp protein in the intestine (Suppl Fig. 7E), reduces intestinal inflammation and stabilizes the gut barrier.

Fexaramine minimally affects bile acid metabolism (synthesis and interconversion) following chronic ethanol administration, but enhances lipid catabolism and represses synthesis of lipids in the liver

Next, we assessed the effect of intestinal FXR activation on bile acid synthesis and composition. Administration of fexaramine increased plasma FGF15 protein concentrations (Fig. 4A) and suppressed hepatic Cyp7a1 protein expression following chronic ethanol feeding (Fig. 4B – 4C). Hepatic expression of *Cyp8b1* mRNA was not modulated by chronic ethanol diet or by fexaramine administration (Fig. 4D). Surprisingly, total plasma bile acids were not significantly different in fexaramine-treated mice after chronic ethanol feeding (Fig. 4E). Similarly, plasma bile acid profiles were not changed dramatically. In mice fed ethanol, fexaramine treatment resulted in a slight increase in plasma omega-MCA and a

small decrease of plasma CA (Fig. 4F). Taken together, an intestine-specific FXR agonist protects from ethanol-induced liver disease in mice. Intestinal FXR activation stabilizes the gut barrier, but affects plasma bile acids only minimally following chronic ethanol administration.

To gain additional insight into the beneficial effect of fexaramine, RNA sequencing of liver tissue was performed (Fig. 5A). Pathway analysis demonstrated activation of multiple pathways in fexaramine-treated mice after ethanol feeding. Differentially regulated pathways included lipid and carbohydrate metabolism (Fig. 5B). Functional analyses of liver transcriptomes revealed that genes involved in triglyceride biosynthesis were downregulated, including fatty acid synthase (*Fasn*), Elongation of long chain fatty acids family member 6 (*Elovl6*) and Lipin1 (*Lpin1*), while nuclear receptor subfamily 1, group D, member 1 (*Nr1d1*, also called *rev-erbA alpha*) as inhibitor of lipogenesis was increased. This is in line with the lower hepatic triglyceride contents following fexaramine treatment. Upregulated genes in the lipolysis pathway including lipoprotein lipase (*Lpl*), contribute to the lipid catabolic effect observed. In addition, fexaramine treatment induced the expression of genes involved in beta-oxidation including pyruvate dehydrogenase kinase, isoenzyme 4 (*Pdk4*) and acyl-CoA thioesterase 2 (*Acot2*) (Fig. 5C). Activation of similar metabolic pathways was observed after overexpression of FGF15 in a model of diet-induced obesity in mice (16). The hepatic fatty acid synthesis–related genes *Srebp1* and *Cidea* were not affected by fexaramine treatment (Suppl Fig. 8). Overall, these findings, combined with minimal changes in bile acid metabolism, are suggestive of a specific role for FGF15 in mediating the metabolic effect of intestinal FXR activation.

The human FGF19-variant M52 increases lipid catabolism, suppresses anabolism of lipids and mitigates alcoholic steatohepatitis

To investigate the proposed role of FGF15 for mediating the beneficial effect of fexaramine, we used adeno-associated virus (AAV) overexpression of a human FGF15 ortholog, the non-tumorigenic FGF19-variant M52 (AAV-M52). AAV-M52 injected mice were protected from ethanol-induced liver injury as demonstrated by lower levels of plasma ALT as compared with control mice injected with GFP expressing AAV (Fig. 6A). AAV-M52 showed a dramatic effect on hepatic triglycerides; AAV-M52 lowered liver triglycerides in isocaloric and ethanol-fed mice to a significantly lower concentration than observed in AAV-GFP injected mice (Fig. 6B – 6D). Hepatic inflammatory markers IL1B and TNF were reduced in AAV-M52 treated mice (Fig. 6E – 6F). Absorption of ethanol and hepatic metabolism of ethanol were not affected by AAV-M52 injection (Suppl. Fig. 9A – 9C). Plasma M52 concentrations were similar in both AAV-M52 injected mouse groups (Suppl. Fig. 9D).

Although overexpression of M52 reduced hepatic Cyp7a1 protein and *Cyp8b1* mRNA expression following ethanol administration (Fig. 7A – 7B), plasma bile acid concentrations were similar in ethanol-fed AAV-M52 and AAV-GFP injected mice (Fig. 7C). The reason for increased conjugated, in particular taurine-conjugated bile acids in isocaloric fed mice injected with AAV-M52 is not known (Fig. 7C). Mice injected with AAV-M52 had markedly lower plasma levels of DCA and TDCA (Fig. 7D). This could contribute to hepatic protection, as DCA has been shown to be toxic to hepatocytes (34, 35).

To further clarify the role of FGF19 in preventing alcoholic steatohepatitis, we compared transcriptional hepatic changes in mice injected with AAV-M52. Notably, overexpression of M52 caused similar transcriptional metabolic changes associated with fexaramine treatment. Specifically, there was a very strong suppression of triglyceride biosynthesis, while lipolysis was activated in M52 overexpressing mice following ethanol feeding (Fig. 7E). The hepatic fatty acid synthesis–related genes *Srebp1* and *Cidea* were not affected by AAV-M52 when alcohol fed groups were compared (Suppl Fig. 9E). Transcriptional changes in lipid metabolism were stronger in mice overexpressing M52 as compared with fexaramine-treated mice. Collectively, these results suggest that intestinal FXR activation and FGF19 overexpression induce similar transcriptional changes involving lipid catabolism that contributes to protection from alcoholic steatohepatitis in mice.

Discussion

Alcoholic liver disease is associated with changes in the intestinal microbiota composition in animal models and humans (36, 37). Although taxonomic changes of the fecal and mucosa-associated microbiota have been characterized in patients with alcohol abuse (5, 6), functional consequences are not well understood. Using metagenomics and bile acid analysis, we demonstrate that chronic alcohol administration is associated with an increase in bacterial choloylglycine hydrolase, which deconjugates bile acids in the intestine of mice. This is accompanied by a lower FGF15 protein secretion from enterocytes in the small intestine and increased hepatic bile acid synthesis. Total plasma and hepatic bile acid concentrations were elevated after chronic ethanol feeding, which likely synergizes with ethanol to cause hepatocyte death.

Bile salt hydrolases of the choloylglycine hydrolase family (EC 3.5.1.24) mediate deconjugation of bile acids (15). Our metagenomic analysis showed increased choloylglycine hydrolase after alcohol feeding. It did not show genomic differences in other enzymes involved in bile acid metabolism in intestinal bacteria. However, we cannot rule out that there are other genes encoded by the intestinal microbiota that contribute to changes in bile acid metabolism associated with chronic ethanol feeding. Alcoholic cirrhotics show increased hepatic bile acid production compared with healthy controls (38) similar to what we demonstrated in alcohol-fed mice in this study. Alcoholic cirrhotics have also been found to have higher fecal concentrations of hepatotoxic DCA and increased secondary to primary bile acid ratios in relation to healthy controls (38). The initiating/central role of the intestinal microbiome in alcohol-related disturbances of bile acid homeostasis has been demonstrated using humanized gnotobiotic mice (39). Germ-free mice transplanted with stool from cirrhotic patients with active alcoholism showed a higher ability to deconjugate and produce secondary bile acids in the stool with subsequent derangements of the bile acid homeostasis in several organs than germ-free mice transplanted with stool from healthy subjects (39) similar to the human subjects themselves (38). This supports the importance of the deconjugating choloylglycine hydrolase family in the development of alcoholic liver disease. In addition to intestinal dysbiosis and bacterial overgrowth (3), a prolonged intestinal transit time associated with alcohol abuse (40) might contribute to increased deconjugation of bile acids.

Non-absorbable antibiotics are known to ameliorate preclinical ethanol-induced liver disease when used as a prevention (41) or intervention (8). Although it is commonly thought that intestinal decontamination reduces intestinal bacterial overgrowth, stabilizes the gut barrier and decreases translocation of bacterial products to the liver (8), broad spectrum antibiotics neomycin and polymyxin B affect bile acid metabolism. Hepatic bile acid synthesis is suppressed and systemic total bile acid concentrations are reduced. Lowering bile acid levels protects from ethanol-induced liver disease, because bile acids are detergents and can be toxic to hepatocytes. In addition, antibiotics cause a shift toward more conjugated, and hence less toxic bile acids. There was also a large decrease in DCA in the presence of antibiotics. DCA is known to be more liver toxic than CA (34). Thus, antibiotics are beneficial for experimental ethanol-induced liver disease by not only stabilizing the intestinal barrier, but also by inhibiting deconjugation of bile acids in the intestine and creating a less hepatotoxic bile acid composition. However, the choice of antibiotics is also important: a cocktail of four antibiotics (ampicillin, neomycin, metronidazole and vancomycin) improved hepatic inflammation and steatosis but did not protect form alcohol-induced increases of ALT/AST (42). Furthermore, the non-absorbable broad-spectrum antibiotic paromomycin failed to improve alcoholic liver disease in patients (43). Since different antibiotics have various effects on systemic bile acid composition and concentrations as well as on ALD in general, antibiotics for future clinical trials have to be carefully selected.

It has been shown that deficiency or inhibition of intestinal FXR (by administration of glycine-beta-MCA, tauro-beta-MCA, or tempol) alleviates obesity and NAFLD in mice (44, 45). However, in alcoholic liver disease, deficiency of FXR worsens liver damage (46, 47), and agonizing FXR activity systemically improves alcoholic liver disease (46). Furthermore, glycine-/tauro-beta-MCA induced changes of the ceramide/Srebp1c/Cidea axis were observed in obesity and NAFLD (30, 45). These pathways do not appear to play a central role in alcoholic liver disease, as there were no significant differences in hepatic expression of Srebp1 or Cidea after alcohol feeding in any of our experiments nor did our pharmacologic interventions change the expression when compared with their alcohol-fed control.

Administration of the systemic FXR agonist WAY-362450 ameliorates ethanol-induced liver disease in mice (46). This protection is partly mediated by suppression of hepatic Cyp2e1 expression (46), which is known to decrease ethanol-induced liver injury (48). Although intestinal FXR activation suppressed hepatic Cyp7a1 expression, it did not suppress systemic bile acids and minimally affected plasma bile acid composition. Fexaramine likely has additional effects beyond targeting bile acid synthesis. One beneficial effect is stabilization of the intestinal barrier, which might account for decreased hepatic inflammation that we observed after ethanol treatment. However, transcriptomics demonstrated a prominent effect on hepatic lipid metabolism, which was mimicked by hepatic overexpression of a FGF19 variant. Consistent with our results, FGF15 has been proposed to be downstream of mitoNEET deficiency in mice, which was associated with protection against alcoholic steatohepatitis (49).

Taken together, metagenomics and bile acid analysis demonstrate functional consequences of intestinal dysbiosis following chronic ethanol administration, including low FGF15

plasma levels, increased hepatic Cyp7a1 expression with disturbed bile acid homeostasis, and changed hepatic lipid metabolism. Modulating dysregulated bile acid signaling improves ethanol-induced liver disease in this preclinical model. Fexaramine and FGF19 are therefore candidate drugs to treat alcoholic steatohepatitis in humans. Although long term toxicity data is currently not available for fexaramine, it has the advantage of being intestinally restricted, thereby potentially avoiding systemic effects seen with systemic FXR agonists such as pruritus (50). NGM282, a non-tumorigenic FGF19 variant similar to M52, has been tested in a Phase 2 clinical trial for primary biliary cholangitis (ClinicalTrials.gov Identifier: NCT02704364) and is currently being tested in a clinical trial for non-alcoholic steatohepatitis (NASH; ClinicalTrials.gov Identifier: NCT02443116). The exact treatment doses of fexaramine and FGF19 variants have still to be determined to achieve the best benefit with a tolerable side effect profile.

Supplementary Material

Refer to Web version on PubMed Central for supplementary material.

Acknowledgments

The manuscript was supported in part by the Deutsche Forschungsgemeinschaft (DFG) grants 7336/1-1 (to P.H.) and HO/ 5690/1-1 (to K.H.), NIH grants R01 AA020703, U01 AA021856, U01 AA24726 (to B.S.), laboratory service agreement with NGM Bio (to B.S.), and by Award Number I01BX002213 from the Biomedical Laboratory Research & Development Service of the VA Office of Research and Development (to B.S.).

Abbreviations

AAV	adeno-associated virus
ADH1	alcohol dehydrogenase 1
ALD	alcoholic liver disease
ALT	alanine aminotransferase
BA	bile acid
CA	cholic acid
CGH	choloylglycine hydrolase
CYP	cytochrome P450 enzyme
DCA	deoxycholic acid
FGF	fibroblast growth factor
FXR	Farnesoid X receptor
IL	interleukin
GFP	green fluorescent protein
LPS	lipopolysaccharide

MCA	muricholic acid
OCLN	occludin
TLR	Toll-like receptor
TNF	tumor necrosis factor
VDAC1	voltage-dependent anion-selective channel protein 1
WT	wild-type

References

1. WHO WHO. Global status report on alcohol and health 2014. 2014.
2. Bull-Otterson L, Feng W, Kirpich I, Wang Y, Qin X, Liu Y, Gobejishvili L, et al. Metagenomic analyses of alcohol induced pathogenic alterations in the intestinal microbiome and the effect of Lactobacillus rhamnosus GG treatment. PLoS One. 2013; 8:e53028. [PubMed: 23326376]
3. Yan AW, Fouts DE, Brandl J, Stärkel P, Torralba M, Schott E, Tsukamoto H, et al. Enteric Dysbiosis Associated with a Mouse Model of Alcoholic Liver Disease. Hepatology. 2011; 53:96–105. [PubMed: 21254165]
4. Mutlu E, Keshavarzian A, Engen P, Forsyth CB, Sikaroodi M, Gillevet P. Intestinal dysbiosis: a possible mechanism of alcohol-induced endotoxemia and alcoholic steatohepatitis in rats. Alcohol Clin Exp Res. 2009; 33:1836–1846. [PubMed: 19645728]
5. Mutlu EA, Gillevet PM, Rangwala H, Sikaroodi M, Naqvi A, Engen PA, Kwasny M, et al. Colonic microbiome is altered in alcoholism. Am J Physiol Gastrointest Liver Physiol. 2012; 302:G966–978. [PubMed: 22241860]
6. Leclercq S, Matamoros S, Cani PD, Neyrinck AM, Jamar F, Starkel P, Windey K, et al. Intestinal permeability, gut-bacterial dysbiosis, and behavioral markers of alcohol-dependence severity. Proc Natl Acad Sci U S A. 2014; 111:E4485–4493. [PubMed: 25288760]
7. Bode JC, Bode C, Heidelbach R, Durr HK, Martini GA. Jejunal microflora in patients with chronic alcohol abuse. Hepatogastroenterology. 1984; 31:30–34. [PubMed: 6698486]
8. Chen P, Stärkel P, Turner JR, Ho SB, Schnabl B. Dysbiosis-induced intestinal inflammation activates TNFRI and mediates alcoholic liver disease in mice. Hepatology. 2015; 61:883–894. [PubMed: 25251280]
9. Parlesak A, Schafer C, Schutz T, Bode JC, Bode C. Increased intestinal permeability to macromolecules and endotoxemia in patients with chronic alcohol abuse in different stages of alcohol-induced liver disease. J Hepatol. 2000; 32:742–747. [PubMed: 10845660]
10. Petrasek J, Bala S, Csak T, Lippai D, Kodys K, Menashy V, Barrieau M, et al. IL-1 receptor antagonist ameliorates inflammasome-dependent alcoholic steatohepatitis in mice. J Clin Invest. 2012; 122:3476–3489. [PubMed: 22945633]
11. Petrasek J, Iracheta-Vellve A, Csak T, Satishchandran A, Kodys K, Kurt-Jones EA, Fitzgerald KA, et al. STING-IRF3 pathway links endoplasmic reticulum stress with hepatocyte apoptosis in early alcoholic liver disease. Proc Natl Acad Sci U S A. 2013; 110:16544–16549. [PubMed: 24052526]
12. Chen P, Torralba M, Tan J, Embree M, Zengler K, Stärkel P, van Pijkeren JP, et al. Supplementation of saturated long-chain fatty acids maintains intestinal eubiosis and reduces ethanol-induced liver injury in mice. Gastroenterology. 2015; 148:203–214. [PubMed: 25239591]
13. Dawson PA, Karpen SJ. Intestinal transport and metabolism of bile acids. J Lipid Res. 2015; 56:1085–1099. [PubMed: 25210150]
14. Schaap FG, Trauner M, Jansen PL. Bile acid receptors as targets for drug development. Nat Rev Gastroenterol Hepatol. 2014; 11:55–67. [PubMed: 23982684]
15. Ridlon JM, Kang DJ, Hylemon PB. Bile salt biotransformations by human intestinal bacteria. J Lipid Res. 2006; 47:241–259. [PubMed: 16299351]

16. Tomlinson E, Fu L, John L, Hultgren B, Huang X, Renz M, Stephan JP, et al. Transgenic mice expressing human fibroblast growth factor-19 display increased metabolic rate and decreased adiposity. Endocrinology. 2002; 143:1741–1747. [PubMed: 11956156]
17. Swann JR, Want EJ, Geier FM, Spagou K, Wilson ID, Sidaway JE, Nicholson JK, et al. Systemic gut microbial modulation of bile acid metabolism in host tissue compartments. Proc Natl Acad Sci U S A. 2011; 108(Suppl 1):4523–4530. [PubMed: 20837534]
18. Kakiyama G, Hylemon PB, Zhou H, Pandak WM, Heuman DM, Kang DJ, Takei H, et al. Colonic inflammation and secondary bile acids in alcoholic cirrhosis. Am J Physiol Gastrointest Liver Physiol. 2014; 306:G929–937. [PubMed: 24699327]
19. Nicolaou KC, Evans RM, Roecker AJ, Hughes R, Downes M, Pfefferkorn JA. Discovery and optimization of non-steroidal FXR agonists from natural product-like libraries. Org Biomol Chem. 2003; 1:908–920. [PubMed: 12929628]
20. Meyer F, Paarmann D, D'Souza M, Olson R, Glass EM, Kubal M, Paczian T, et al. The metagenomics RAST server - a public resource for the automatic phylogenetic and functional analysis of metagenomes. BMC Bioinformatics. 2008; 9:386. [PubMed: 18803844]
21. Alnouti Y, Csanaky IL, Klaassen CD. Quantitative-profiling of bile acids and their conjugates in mouse liver, bile, plasma, and urine using LC-MS/MS. J Chromatogr B Analyt Technol Biomed Life Sci. 2008; 873:209–217.
22. Huang J, Bathena SP, Csanaky IL, Alnouti Y. Simultaneous characterization of bile acids and their sulfate metabolites in mouse liver, plasma, bile, and urine using LC-MS/MS. J Pharm Biomed Anal. 2011; 55:1111–1119. [PubMed: 21530128]
23. Wang L, Hartmann P, Haimerl M, Bathena SP, Sjowall C, Almer S, Alnouti Y, et al. Nod2 deficiency protects mice from cholestatic liver disease by increasing renal excretion of bile acids. J Hepatol. 2014; 60:1259–1267. [PubMed: 24560660]
24. Fang S, Suh JM, Reilly SM, Yu E, Osborn O, Lackey D, Yoshihara E, et al. Intestinal FXR agonism promotes adipose tissue browning and reduces obesity and insulin resistance. Nat Med. 2015; 21:159–165. [PubMed: 25559344]
25. Dobin A, Davis CA, Schlesinger F, Drenkow J, Zaleski C, Jha S, Batut P, et al. STAR: ultrafast universal RNA-seq aligner. Bioinformatics. 2013; 29:15–21. [PubMed: 23104886]
26. Trapnell C, Hendrickson DG, Sauvageau M, Goff L, Rinn JL, Pachter L. Differential analysis of gene regulation at transcript resolution with RNA-seq. Nat Biotechnol. 2013; 31:46–53. [PubMed: 23222703]
27. Roberts A, Pimentel H, Trapnell C, Pachter L. Identification of novel transcripts in annotated genomes using RNA-Seq. Bioinformatics. 2011; 27:2325–2329. [PubMed: 21697122]
28. Jones BV, Begley M, Hill C, Gahan CG, Marchesi JR. Functional and comparative metagenomic analysis of bile salt hydrolase activity in the human gut microbiome. Proc Natl Acad Sci U S A. 2008; 105:13580–13585. [PubMed: 18757757]
29. Inagaki T, Moschetta A, Lee YK, Peng L, Zhao G, Downes M, Yu RT, et al. Regulation of antibacterial defense in the small intestine by the nuclear bile acid receptor. Proc Natl Acad Sci U S A. 2006; 103:3920–3925. [PubMed: 16473946]
30. Jiang C, Xie C, Li F, Zhang L, Nichols RG, Krausz KW, Cai J, et al. Intestinal farnesoid X receptor signaling promotes nonalcoholic fatty liver disease. J Clin Invest. 2015; 125:386–402. [PubMed: 25500885]
31. Inagaki T, Choi M, Moschetta A, Peng L, Cummins CL, McDonald JG, Luo G, et al. Fibroblast growth factor 15 functions as an enterohepatic signal to regulate bile acid homeostasis. Cell Metab. 2005; 2:217–225. [PubMed: 16213224]
32. Studer E, Zhou X, Zhao R, Wang Y, Takabe K, Nagahashi M, Pandak WM, et al. Conjugated bile acids activate the sphingosine-1-phosphate receptor 2 in primary rodent hepatocytes. Hepatology. 2012; 55:267–276. [PubMed: 21932398]
33. Arroyo V, Moreau R, Kamath PS, Jalan R, Gines P, Nevens F, Fernandez J, et al. Acute-on-chronic liver failure in cirrhosis. Nat Rev Dis Primers. 2016; 2:16041. [PubMed: 27277335]
34. Song P, Zhang Y, Klaassen CD. Dose-response of five bile acids on serum and liver bile Acid concentrations and hepatotoxicty in mice. Toxicol Sci. 2011; 123:359–367. [PubMed: 21747115]

35. Delzenne NM, Calderon PB, Taper HS, Roberfroid MB. Comparative hepatotoxicity of cholic acid, deoxycholic acid and lithocholic acid in the rat: in vivo and in vitro studies. Toxicol Lett. 1992; 61:291–304. [PubMed: 1641875]
36. Betrapally NS, Gillevet PM, Bajaj JS. Changes in the Intestinal Microbiome and Alcoholic and Nonalcoholic Liver Diseases: Causes or Effects? Gastroenterology. 2016; 150:1745–1755. e1743. [PubMed: 26948887]
37. Massey VL, Beier JI, Ritzenthaler JD, Roman J, Arteel GE. Potential Role of the Gut/Liver/Lung Axis in Alcohol-Induced Tissue Pathology. Biomolecules. 2015; 5:2477–2503. [PubMed: 26437442]
38. Bajaj JS, Kakiyama G, Zhao D, Takei H, Fagan A, Hylemon P, Zhou H, et al. Continued Alcohol Misuse in Human Cirrhosis is Associated with an Impaired Gut-Liver Axis. Alcohol Clin Exp Res. 2017
39. Kang DJ, Hylemon PB, Gillevet PM, Sartor RB, Betrapally NS, Kakiyama G, Sikaroodi M, et al. Gut microbial composition can differentially regulate bile acid synthesis in humanized mice. Hepatology Communications. 2017; 1:61–70. [PubMed: 29404434]
40. Bode C, Kolepke R, Schafer K, Bode JC. Breath hydrogen excretion in patients with alcoholic liver disease--evidence of small intestinal bacterial overgrowth. Z Gastroenterol. 1993; 31:3–7. [PubMed: 8447153]
41. Adachi Y, Moore LE, Bradford BU, Gao W, Thurman RG. Antibiotics prevent liver injury in rats following long-term exposure to ethanol. Gastroenterology. 1995; 108:218–224. [PubMed: 7806045]
42. Lowe PP, Gyongyosi B, Satishchandran A, Iracheta-Vellve A, Ambade A, Kodys K, Catalano D, et al. Alcohol-related changes in the intestinal microbiome influence neutrophil infiltration, inflammation and steatosis in early alcoholic hepatitis in mice. PLoS One. 2017; 12:e0174544. [PubMed: 28350851]
43. Bode C, Schafer C, Fukui H, Bode JC. Effect of treatment with paromomycin on endotoxemia in patients with alcoholic liver disease--a double-blind, placebo-controlled trial. Alcohol Clin Exp Res. 1997; 21:1367–1373. [PubMed: 9394106]
44. Li F, Jiang C, Krausz KW, Li Y, Albert I, Hao H, Fabre KM, et al. Microbiome remodelling leads to inhibition of intestinal farnesoid X receptor signalling and decreased obesity. Nat Commun. 2013; 4:2384. [PubMed: 24064762]
45. Jiang C, Xie C, Lv Y, Li J, Krausz KW, Shi J, Brocker CN, et al. Intestine-selective farnesoid X receptor inhibition improves obesity-related metabolic dysfunction. Nat Commun. 2015; 6:10166. [PubMed: 26670557]
46. Wu W, Zhu B, Peng X, Zhou M, Jia D, Gu J. Activation of farnesoid X receptor attenuates hepatic injury in a murine model of alcoholic liver disease. Biochem Biophys Res Commun. 2014; 443:68–73. [PubMed: 24269813]
47. Manley S, Ni HM, Williams JA, Kong B, DiTacchio L, Guo G, Ding WX. Farnesoid X receptor regulates forkhead Box O3a activation in ethanol-induced autophagy and hepatotoxicity. Redox Biol. 2014; 2:991–1002. [PubMed: 25460735]
48. Lu Y, Zhuge J, Wang X, Bai J, Cederbaum AI. Cytochrome P450 2E1 contributes to ethanol-induced fatty liver in mice. Hepatology. 2008; 47:1483–1494. [PubMed: 18393316]
49. Hu X, Jogasuria A, Wang J, Kim C, Han Y, Shen H, Wu J, et al. MitoNEET Deficiency Alleviates Experimental Alcoholic Steatohepatitis in Mice by Stimulating Endocrine Adiponectin-Fgf15 Axis. J Biol Chem. 2016; 291:22482–22495. [PubMed: 27573244]
50. Neuschwander-Tetri BA, Loomba R, Sanyal AJ, Lavine JE, Van Natta ML, Abdelmalek MF, Chalasani N, et al. Farnesoid X nuclear receptor ligand obeticholic acid for non-cirrhotic, non-alcoholic steatohepatitis (FLINT): a multicentre, randomised, placebo-controlled trial. Lancet. 2015; 385:956–965. [PubMed: 25468160]

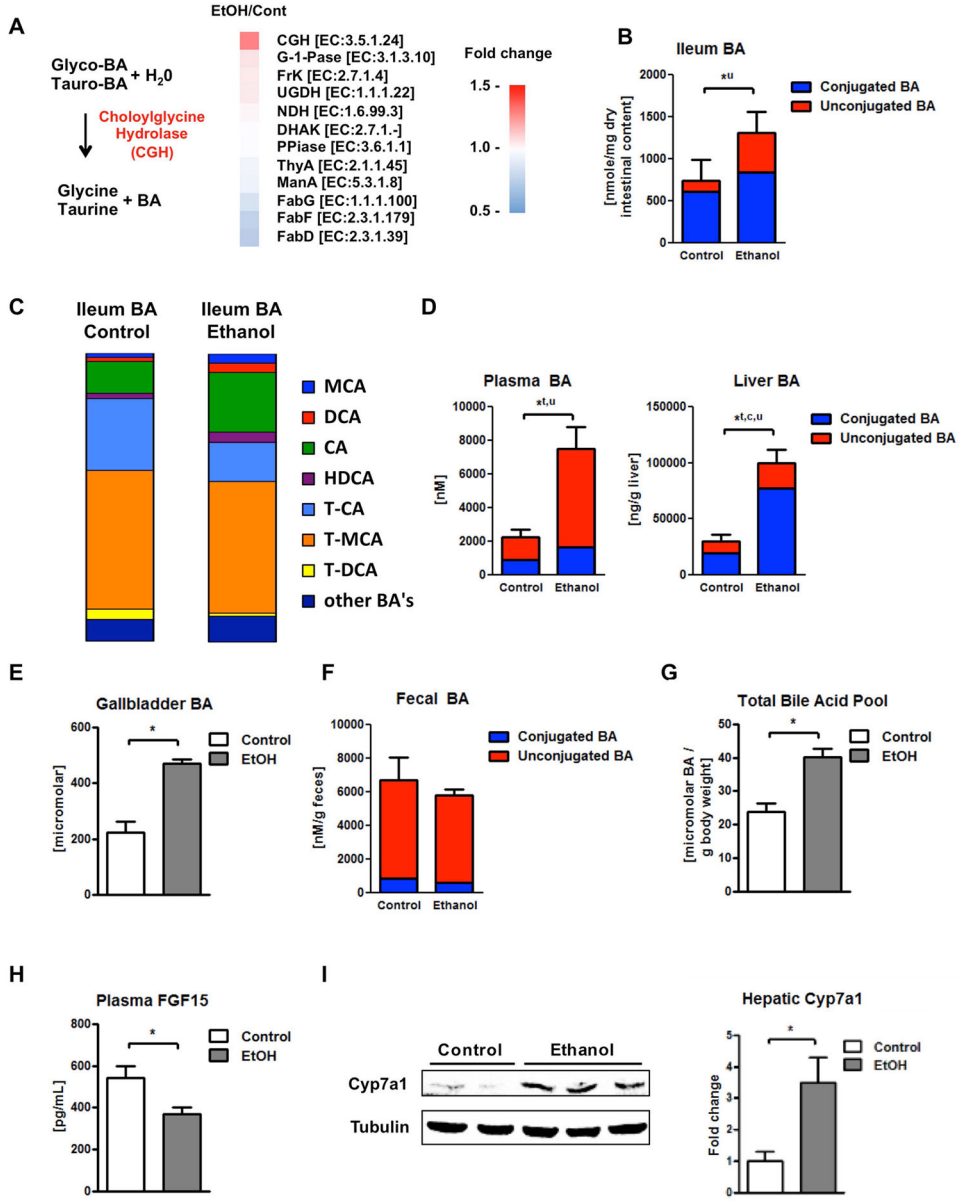

Figure 1. Administration of ethanol leads to elevated levels of unconjugated bile acids in the intestine and plasma, and augmented Cyp7a1 protein expression and conjugated bile acids in the liver

C57BL/6 mice were fed an oral control diet (n=5–12) or ethanol diet (n=8–18) for 8 weeks. (A) Metagenomic sequencing revealed an increased proportion of bacterial genomic DNA containing choloylglycine hydrolase (CGH), a major enzyme for deconjugation (deamidation) of conjugated bile acids, after ethanol feeding. Other metabolic enzymes are listed for comparison. Bacterial genomic DNA for FabG, FabF, and FabD, genes involved in fatty acid metabolism, were found decreased after alcohol administration (12). (B) Bile acid concentrations in ileal contents. Unconjugated bile acid levels are significantly higher between ethanol and control fed mice. (C) Bile acid composition ratio in ileal contents. (D) Bile acid concentrations in plasma (left; significant differences with respect to unconjugated

and total bile acids), liver (right; significant differences with respect to unconjugated, conjugated and total bile acids). (E) Bile acid concentrations in gallbladder. (F) Bile acid concentrations in feces. (G) Total bile acid pool. (H) Plasma FGF15 concentration. (I) Immunoblot analysis of hepatic Cyp7a1. $*P < 0.05$. Abbreviations: Genes: CGH, Choloylglycine hydrolase; DHAK, Dihydroxyacetone kinase, C-terminal domain; EC, Enzyme Commission Number; FabD, [acyl-carrier-protein] S-malonyltransferase; FabF, 3-oxoacyl-[acyl-carrier-protein] synthase II; FabG, 3-oxoacyl-[acyl-carrier protein] reductase; FrK, Fructokinase; G-1Pase, Glucose-1-phosphatase; ManA, Mannose-6-phosphate isomerase; NDH, NADH dehydrogenase; PPiase, Inorganic pyrophosphatase; ThyA, Thymidylate synthase; UGDH, UDPglucose 6-dehydrogenase. Bile acids: BA, bile acid; c, conjugated; CA, cholic acid; DCA, deoxycholic acid; HDCA, hyodeoxycholic acid; MCA, muricholic acid; T-CA, taurocholic acid; T-DCA, taurodeoxycholic acid; T-MCA, tauromuricholic acid; t, total; u, unconjugated. Cyp7a1, cholesterol 7a-hydroxylase; EtOH, ethanol; FGF15, fibroblast growth factor 15.

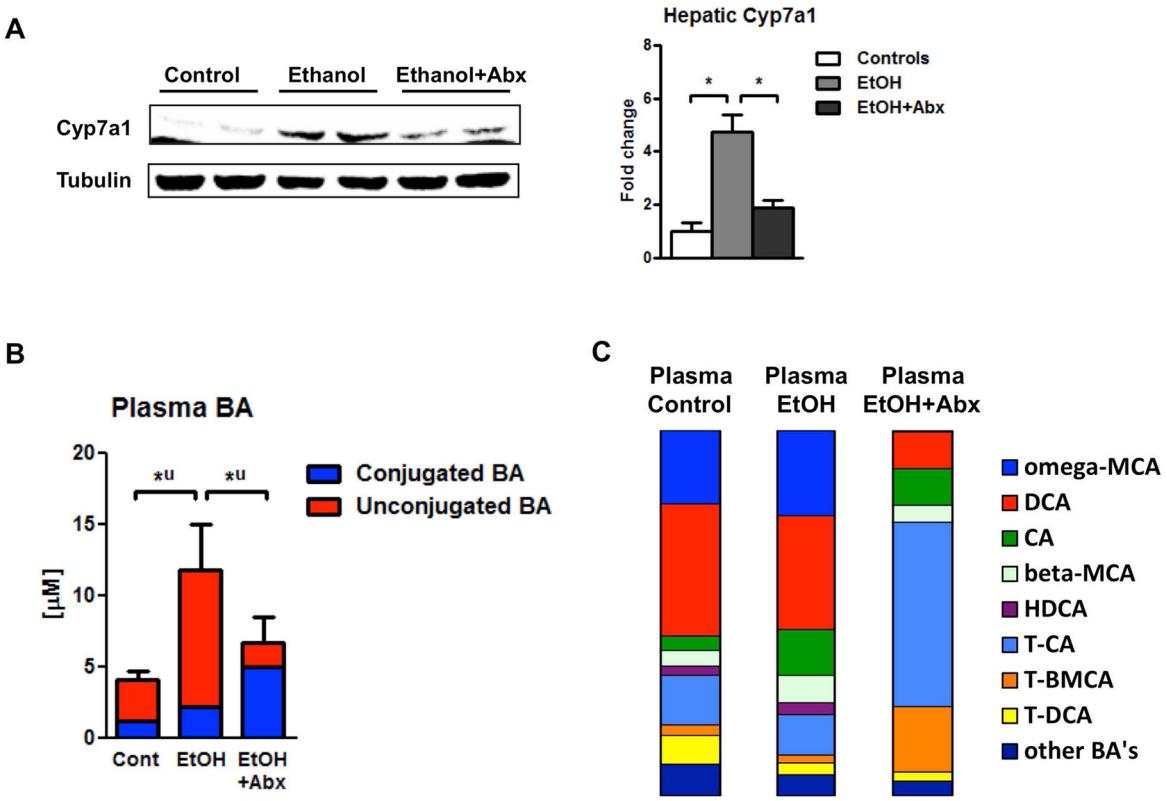

Figure 2. Disruption of bile acid homeostasis depends on intestinal microbiota in alcoholic liver disease

C57BL/6 mice were fed an oral control diet or ethanol diet for 8 weeks (n=7–9). Antibiotics polymyxin B and neomycin were administered during the last 4 weeks of feeding. (A) Immunoblot analysis of hepatic Cyp7a1. (B) Plasma bile acid levels. (C) Plasma bile acid composition ratio. *$P < 0.05$. Abbreviations: Abx, antibiotics; BA, bile acid; CA, cholic acid; Cont, control; Cyp7a1, cholesterol 7a-hydroxylase; DCA, deoxycholic acid; EtOH, ethanol; HDCA, hyodeoxycholic acid; MCA, muricholic acid; T-BMCA, tauro-beta-muricholic acid; T-CA, taurocholic acid; T-DCA, taurodeoxycholic acid; T-MCA, tauromuricholic acid; u, unconjugated.

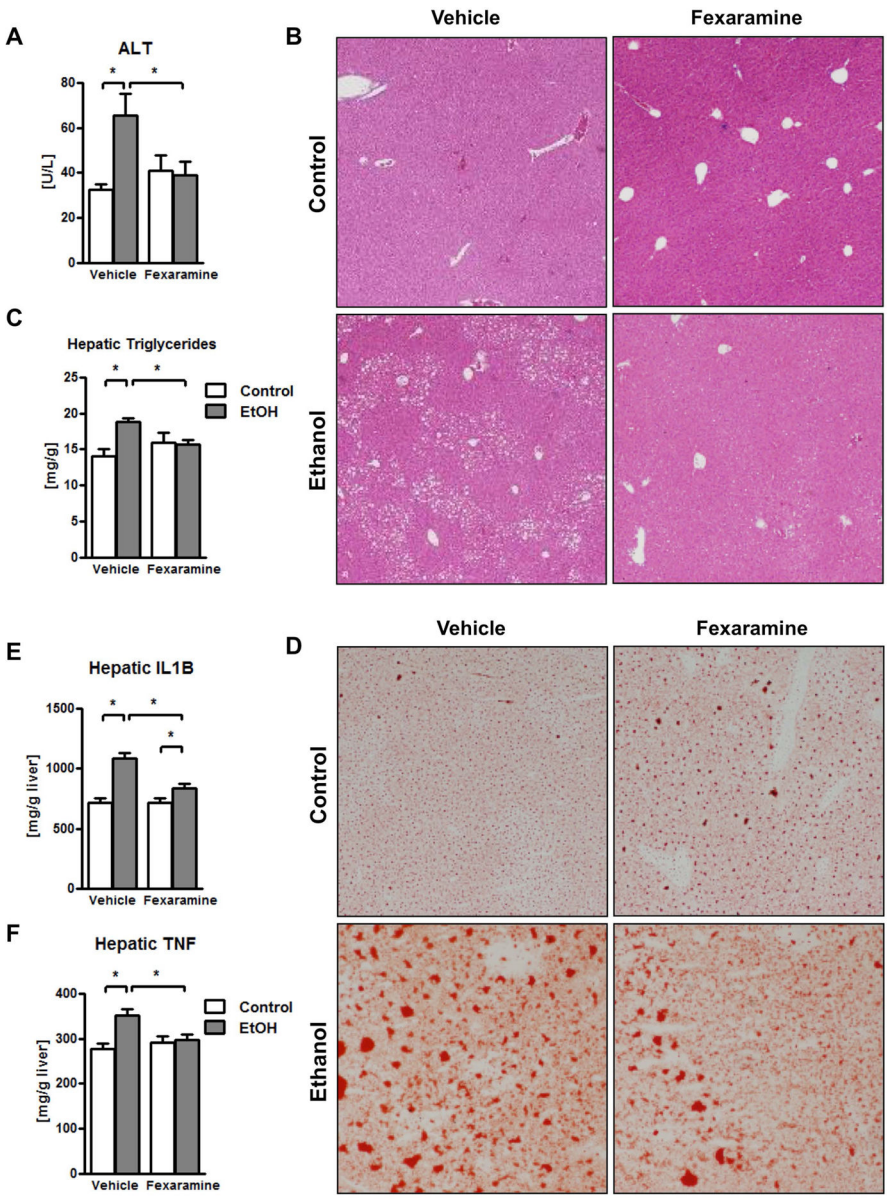

Figure 3. The intestinal FXR agonist fexaramine ameliorates alcoholic liver disease

C57BL/6 mice were fed an oral control diet (n=5–10) or ethanol diet (n=12–17), and also given vehicle (corn oil) or fexaramine for 8 weeks. (A) Plasma levels of ALT. (B) Representative liver sections after hematoxylin and eosin staining. (C) Hepatic triglyceride content. (D) Representative Oil Red O-stained liver sections. (E) Hepatic concentrations of IL1B protein. (F) Hepatic concentrations of TNF protein. $*P < 0.05$. Abbreviations: ALT, alanine aminotransferase; IL1B, interleukin-1 beta; TNF, tumor necrosis factor.

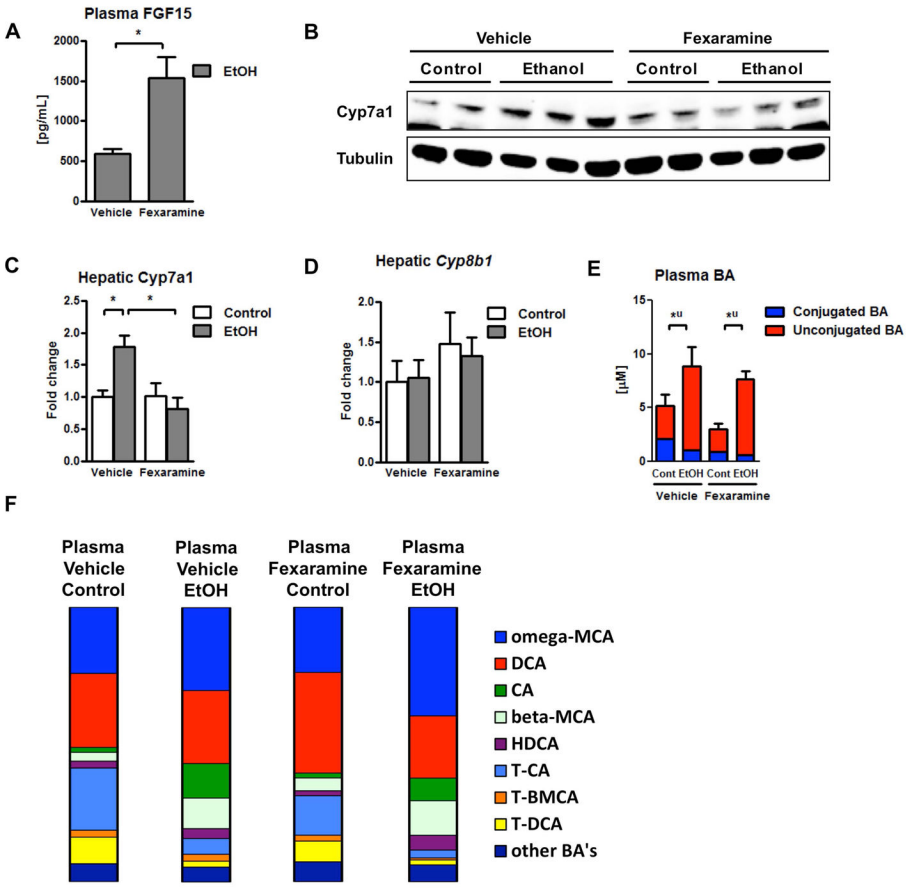

Figure 4. Fexaramine minimally affects bile acid metabolism

C57BL/6 mice were fed an oral control diet (n=5–8) or ethanol diet (n=12–16), and also given vehicle (corn oil) or fexaramine for 8 weeks. (A) Plasma FGF15 concentration. (B, C) Immunoblot analysis of hepatic Cyp7a1. (D) Hepatic expression of *Cyb8b1* mRNA. (E) Plasma bile acid levels. (F) Plasma bile acid composition ratio. **P* < 0.05. Abbreviations: BA, bile acid; CA, cholic acid; Cont, control; Cyp7a1, cholesterol 7a-hydroxylase; Cyp8b1, sterol 12α-hydroxylase; DCA, deoxycholic acid; EtOH, ethanol; FGF15, fibroblast growth factor 15; HDCA, hyodeoxycholic acid; MCA, muricholic acid; T-BMCA, tauro-beta-muricholic acid; T-CA, taurocholic acid; T-DCA, taurodeoxycholic acid; T-MCA, tauromuricholic acid; u, unconjugated.

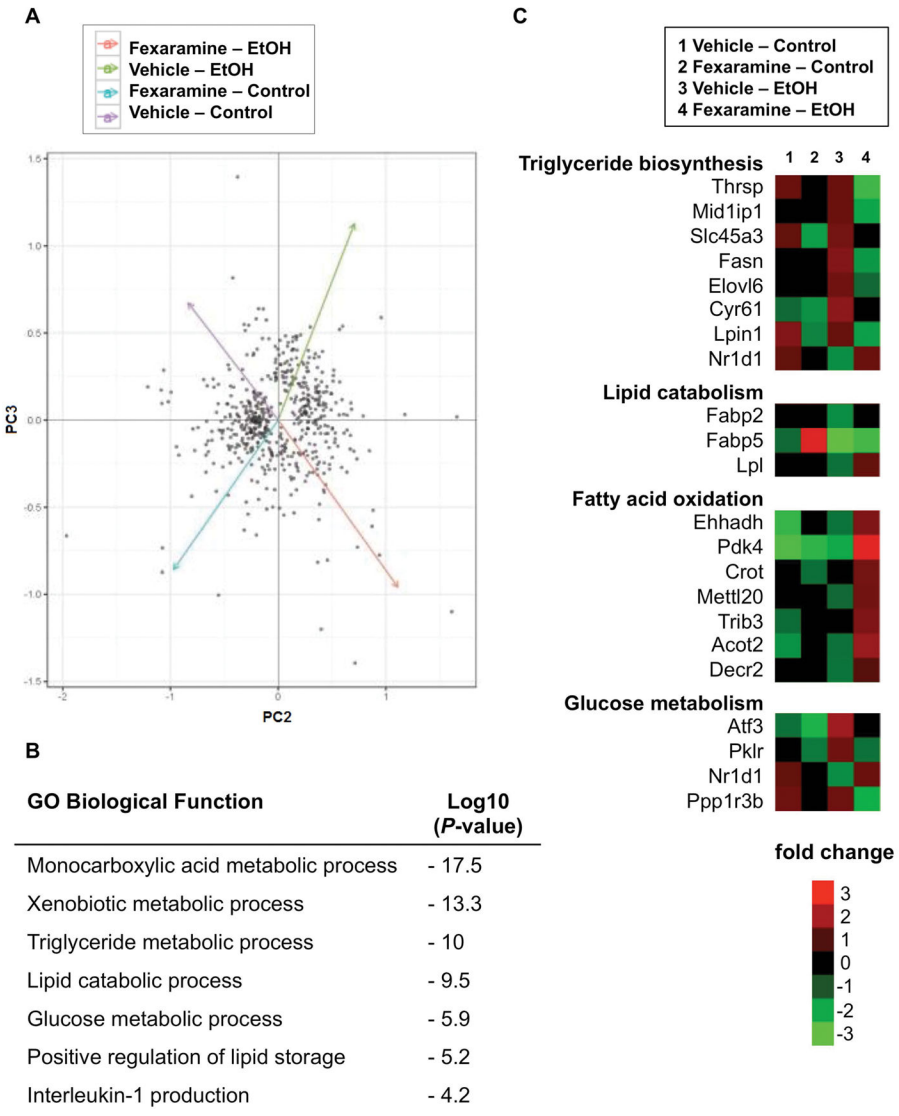

B

GO Biological Function	Log10 (*P*-value)
Monocarboxylic acid metabolic process	- 17.5
Xenobiotic metabolic process	- 13.3
Triglyceride metabolic process	- 10
Lipid catabolic process	- 9.5
Glucose metabolic process	- 5.9
Positive regulation of lipid storage	- 5.2
Interleukin-1 production	- 4.2

Figure 5. Fexaramine shows lipocatabolic and anti-lipogenic effects following chronic ethanol administration

C57BL/6 mice were fed an oral control diet (n=6–8) or ethanol diet (n=12–18), and also given vehicle (corn oil) or fexaramine for 8 weeks. RNASeq libraries were prepared from two biological replicates for each experimental condition. (A) Principal component analysis (PCA) of RNAseq of significantly changed genes expressed in the liver, 2nd and 3rd components indicated by the x and y axes respectively. (B) Functional annotation of altered gene categories in vehicle vs fexaramine-treated mice after chronic ethanol feeding identified by gene ontology (GO). (C) Heat map of gene expression changes in selected metabolic pathway. Fold change denotes the change of gene expression for a certain group in relation to the expression average of all four treatment groups. Abbreviations: Acot2, Acyl-coenzyme A thioesterase 2; Atf3, Activating transcription factor 3; Crot, Carnitine O-octanoyltransferase; Decr2, 2,4-dienoyl-CoA reductase; Ehhadh, Enoyl-CoA hydratase and 3-hydroxyacyl CoA dehydrogenase; Elovl6, Elongation of very long chain fatty acids

protein 6; Fabp2/5, Fatty acid binding protein 2/5; Fasn, Fatty acid synthase; Lpin1, Lipin 1; Lpl, lipoprotein lipase; Mettl20, Methyltransferase like 20; Mid1ip1, Midline 1 interacting protein 1; Nr1d1, Nuclear receptor subfamily 1, group D, member 1; Pdk4, Pyruvate dehydrogenase kinase, isoenzyme 4; Ppp1r3b, Protein phosphatase 1, regulatory subunit 3B; Slc45a3, Solute carrier family 45 member 3; Trib3, Tribbles pseudokinase 3; Thrsp, Thyroid hormone-inducible hepatic protein.

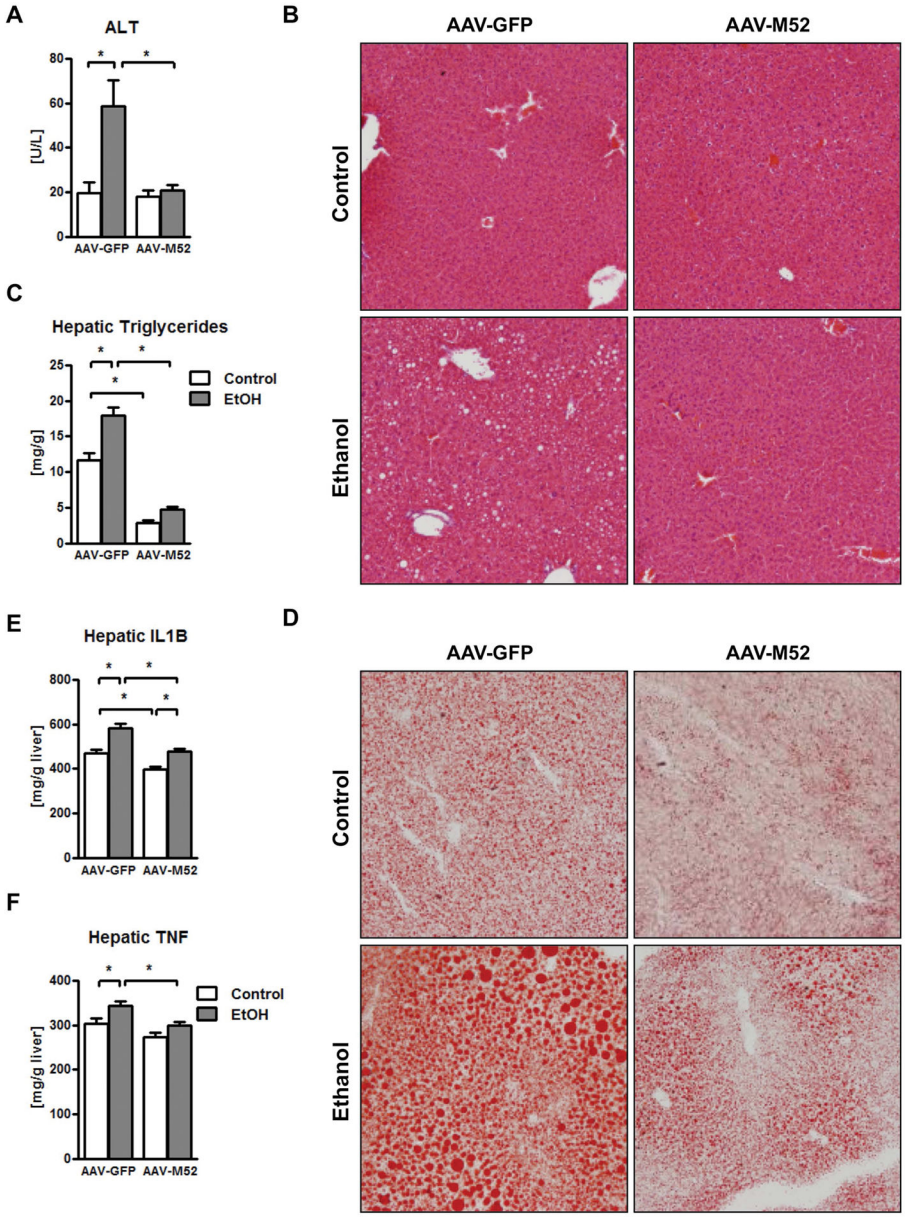

Figure 6. FGF19-variant M52 protects from alcoholic liver disease

C57BL/6 mice were fed an oral control diet (n=5–11) or ethanol diet (n=13–19). Mice were injected adeno-associated virus with FGF19-variant M52 (AAV-M52) or AAV-GFP as control 3 weeks after liquid diet feeding was started. (A) Plasma levels of ALT. (B) Representative liver sections after hematoxylin and eosin staining. (C) Hepatic triglyceride content. (D) Representative Oil Red O-stained liver sections. (E) Hepatic concentrations of IL1B protein. (F) Hepatic concentrations of TNF protein. $*P < 0.05$. Abbreviations: AAV, adeno-associated virus; ALT, alanine aminotransferase; GFP, green fluorescent protein; IL1B, interleukin-1 beta; M52, fibroblast growth factor 19-variant M52; TNF, tumor necrosis factor.

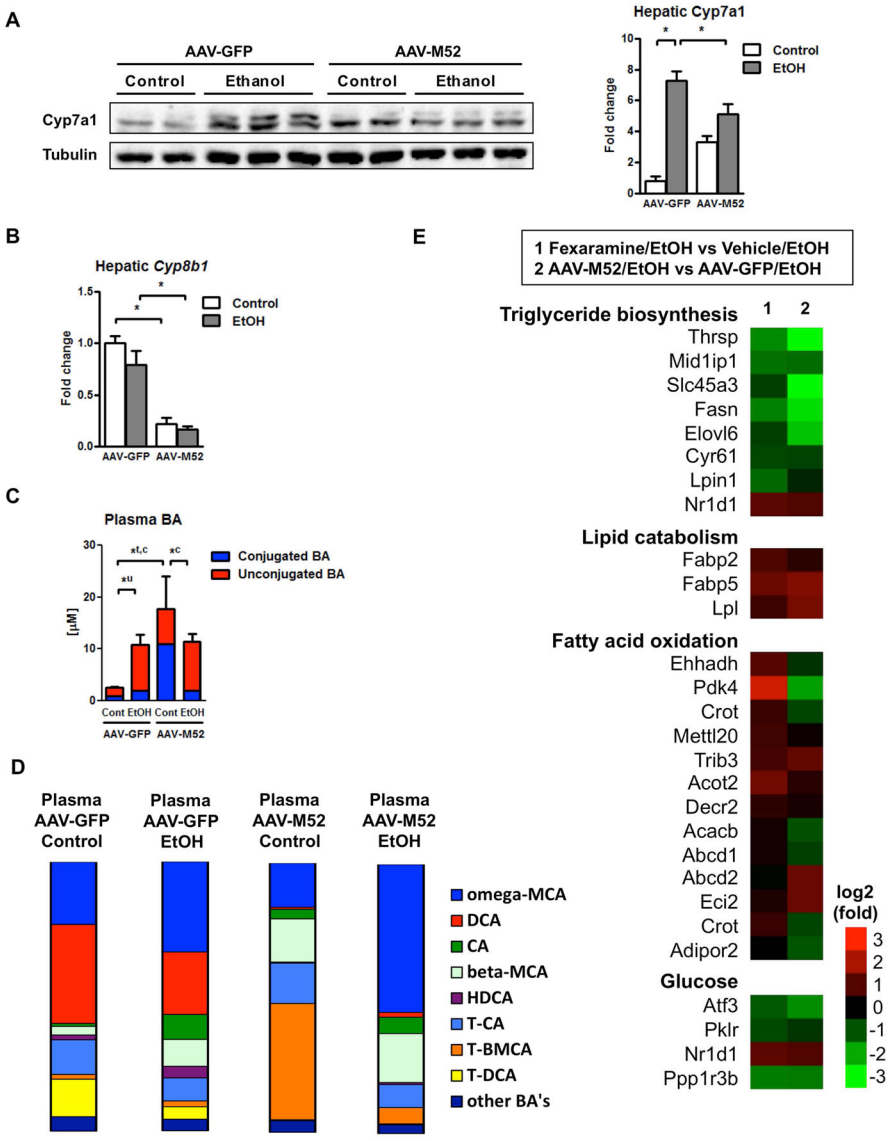

Figure 7. FGF19-variant M52 results in lipocatabolic and anti-lipogenic hepatic gene expression following chronic ethanol administration

C57BL/6 mice were fed an oral control diet (n=5–6) or ethanol diet (n=13–15). Mice were injected adeno-associated virus with FGF19-variant M52 (AAV-M52) or AAV-GFP as control 3 weeks after liquid diet feeding was started. (A) Immunoblot analysis of hepatic Cyp7a1. (B) Hepatic expression of *Cyb8b1* mRNA. (C) Plasma bile acid levels. (D) Plasma bile acid composition ratio. (E) RNASeq libraries were prepared from two biological replicates for each experimental condition. Heatmap of expression changes of hepatic genes in selected metabolic pathways. Fexaramine vs vehicle treated mice after ethanol feeding (left) and mice injected with AAV-M52 vs AAV-GFP after ethanol feeding (right). $*P < 0.05$. Abbreviations: AAV, adeno-associated virus; BA, bile acid; CA, cholic acid; c, conjugated; Cont, control; Cyp7a1, cholesterol 7a-hydroxylase; Cyp8b1, sterol 12α-hydroxylase; DCA, deoxycholic acid; EtOH, ethanol; FGF15, fibroblast growth factor 15; GFP, green fluorescent protein; HDCA, hyodeoxycholic acid; M52, fibroblast growth factor 19-variant

M52; MCA, muricholic acid; T-BMCA, tauro-beta-muricholic acid; T-CA, taurocholic acid; T-DCA, taurodeoxycholic acid; T-MCA, tauromuricholic acid; t, total; u, unconjugated. Genes: Abcd1/2, ATP binding cassette subfamily D member 1/2; Acacb, Acetyl-CoA carboxylase beta; Acot2, Acyl-coenzyme A thioesterase 2; Adipor2, Adiponectin receptor protein 2; Atf3, Activating transcription factor 3; Crot, Carnitine O-octanoyltransferase; Cyr61, Cysteine rich angiogenic inducer 61; Decr2, 2,4-dienoyl-CoA reductase; Eci1, Enoyl-CoA delta isomerase 1; Ehhadh, Enoyl-CoA hydratase and 3-hydroxyacyl CoA dehydrogenase; Elovl6, Elongation of very long chain fatty acids protein 6; Fabp2/5, Fatty acid binding protein 2/5; Fasn, Fatty acid synthase; Lpin1, Lipin 1; Lpl, lipoprotein lipase; Mettl20, Methyltransferase like 20; Mid1ip1, Midline 1 interacting protein 1; Nr1d1, Nuclear receptor subfamily 1, group D, member 1; Pdk4, Pyruvate dehydrogenase kinase, isoenzyme 4; Pklr, Pyruvate kinase liver and red blood cell; Ppp1r3b, Protein phosphatase 1, regulatory subunit 3B; Slc45a3, Solute carrier family 45 member 3; Trib3, Tribbles pseudokinase 3; Thrsp, Thyroid hormone-inducible hepatic protein.